

# Materials Advances

Accepted Manuscript

This article can be cited before page numbers have been issued, to do this please use: B. Sharma, A. Sahi, J. Dhau, A. Kaushik, R. Kumar and G. R. Chaudhary, *Mater. Adv.*, 2024, DOI: 10.1039/D4MA00717D.



This is an Accepted Manuscript, which has been through the Royal Society of Chemistry peer review process and has been accepted for publication.

Accepted Manuscripts are published online shortly after acceptance, before technical editing, formatting and proof reading. Using this free service, authors can make their results available to the community, in citable form, before we publish the edited article. We will replace this Accepted Manuscript with the edited and formatted Advance Article as soon as it is available.

You can find more information about Accepted Manuscripts in the [Information for Authors](#).

Please note that technical editing may introduce minor changes to the text and/or graphics, which may alter content. The journal's standard [Terms & Conditions](#) and the [Ethical guidelines](#) still apply. In no event shall the Royal Society of Chemistry be held responsible for any errors or omissions in this Accepted Manuscript or any consequences arising from the use of any information it contains.

## Recycling Waste Aluminium Foil to Bio-Acceptable Nano Photocatalyst [Aluminium oxide (Al<sub>2</sub>O<sub>3</sub>) & Aluminium oxyhydroxide (AlOOH)]; Dye Degradation as Proof-of-Concept

Bunty Sharma<sup>a§</sup>, Arshdeep Sahi<sup>b§</sup>, Jaspreet Dhau<sup>a</sup>, Ajeet Kaushik<sup>c</sup>, Rajeev Kumar<sup>b\*</sup> and Ganga Ram Chaudhary<sup>d,e\*</sup>

<sup>a</sup> *Research and Development, Molekule Inc., Lakeland, Florida, USA*

<sup>b</sup> *Department of Environment Studies, Panjab University, Chandigarh, 160014 India*

<sup>c</sup> *NanoBioTech Laboratory, Department of Environmental Engineering, Florida Polytechnic University, Lakeland, FL, USA*

<sup>d</sup> *Department of Chemistry and Center for Advance Study in Chemistry, Chandigarh, India*

<sup>e</sup> *Sophisticated Analytical Instrumentation Laboratory (SAIF)/Central Instrumentation Laboratory (CIL), Panjab University, Chandigarh, 160014, India*

<sup>§</sup> Both have contributed equally.

\* Corresponding authors: (Rajeev Kumar and Ganga Ram Chaudhary)

### Abstract:

The surge in the world's population resulting from urbanization and industrialization has led to a significant uptick in water and soil pollution. Aligning with the United Nations goals of sustainability, it is recommended to earnestly investigate innovative methods for repurposing waste into beneficial materials and effective catalysts that are compatible with ecosystems and capable of efficiently decomposing dyes. Additionally, aligning with the objectives of a sustainable society, this study serves as a prototype for repurposing discarded aluminium foil-an everyday single-use material contributing to landfill accumulation-into aluminium oxide (Al<sub>2</sub>O<sub>3</sub>) and aluminium oxyhydroxide (AlOOH) nanocatalysts, intended for efficient photodegradation applications. Both Al<sub>2</sub>O<sub>3</sub> and AlOOH nano-systems were synthesized using a well-optimized chemistry route. The developed nano-systems were characterized using FTIR, EDX mapping, XRD, FE-SEM, and TGA/DTA which found the bonds, composition, structure, morphology of the particles, and thermal stability, respectively. These particles are used for the degradation of cationic Methylene Blue (MB) in neutral (pH 7), basic (pH 9), and acidic (pH 5) mediums. Liquid chromatography mass spectrometry (LC-MS) was performed to check the MB intermediate product formation on photodegradation. The findings suggest that exposing cationic MB to light in neutral pH conditions with Al<sub>2</sub>O<sub>3</sub> is highly effective, with a dye degradation rate of 99.29%. Exposing MB to the dark in neutral conditions with AlOOH is the least effective, with a dye degradation rate of 6.64%. As the pH is made more acidic and/or basic, the effectiveness of Al<sub>2</sub>O<sub>3</sub> and AlOOH also slightly changes. The outcomes related with both reusability and toxicity studies also proven positive acceptability of the developed systems. The degradation using both compounds led to more germination when compared to MB, and both compounds showed outstanding reusability. The research emphasizes the importance of sustainable materials synthesis and offers valuable insights for the development of efficient photocatalysts tailored for specific environmental conditions in the context of dye degradation.



**Keywords:** Waste Aluminium Foil, Methylene Blue, Photocatalysis, Aluminium oxide, Aluminium oxyhydroxide

## 1. Introduction:

Over the past century, the global population has surged from 2.2 billion individuals to 7.9 billion, showing an exponential growth trend due to technological advancement and industrialization. Consequently, this expansion has led to the generation of new pollution sources including solid waste pollution in water. The interconnection between population growth and pollution is clear in the widespread increase in single-use products and other disposable packaging materials. The global pandemic has further propelled industrial demand for single-use materials. Since the COVID-19 pandemic (2020), single-use food packaging containers and wrappers have drastically increased [1,2]. As the demand for these products rises, environmental degradation caused by the production of raw materials and the disposal of old materials also escalates. One such waste-generating, single-use pollutant, includes aluminium foil, whose development is intricately linked with industrialization and a rise in food production. Aluminium foil is an integral part of the packaging industry including the preparation of food and several other industrial applications, nevertheless, aluminium disposal poses a sizeable threat to the environment [3]. Since the lockdown in 2020, there has been a 54% increase in food wrapper use globally [1,2]. Aluminum pollution stems from the widespread improper disposal of aluminium-based materials and is linked to both natural and anthropogenic sources. If aluminium is disposed of incorrectly, it creates environmental degradation regardless of whether it decomposes or not. If the foil decomposes or breaks down, it will introduce new chemical compounds to the environment, causing environmental pollution. However, if the foil does not break down, it further causes solid waste pollution to waterways and otherwise. These anthropogenic sources have a considerable impact on environmental and human health.

When foil is correctly disposed of, it ends up in landfills, incinerators, or recycling plants. However, foil has a long decomposition cycle, causing it to be persistent in municipal solid waste facilities for extended periods [4]. The incineration of foil causes increased air pollution and further causes soil and water pollution [5]. Aluminium in landfills poses equally threatening environmental problems by giving rise to unwanted heat generated by chemical reactions in



decomposition, production of liquid leachate, and the generation of gases such as hydrogen, hydrogen sulfide, carbon monoxide, and ammonia which cause considerable impacts to human health [5,6]. Trends indicate an increase in diseases such as Alzheimer's disease, autism, epilepsy, and other neurological diseases associated with these pollutants [7]. Aluminum is also challenging to recycle, as the foil that is finally brought to recycling facilities is generally torn and wrinkled or contaminated with leftover food debris. Compromised foil cannot be recycled. Solid aluminum waste is a concern for municipal solid waste facilities and environmental health and safety management due to its persistent nature, however, if waste foil is treated to remove contaminants, then it can be used to synthesize aluminum particles which can be used multifariously in dye degradation, absorbing, dye binding, desiccating agent, drug delivery, antimicrobial potential and photocatalysts in waterways [8-10]. It is reported in the literature that various metal oxides and nanocomposites were prepared and used for sensing, energy storage and removal of pollutants in water [11-13]. Studies have shown promising results of  $\text{Al}_2\text{O}_3$  and  $\text{AlOOH}$  particles in the degradation of organic pollutants for treatment of contaminated water [14]. Specifically, many photodegradation reactions have been performed using  $\text{Al}_2\text{O}_3$  as a photocatalyst. A recently published review article meticulously scrutinises recent developments in  $\text{Al}_2\text{O}_3$ -based materials, highlighting their efficacy in both organic dye adsorption and degradation [15]. For example, Anna *et al.*, have used these particles as a photocatalyst for degradation of methylene blue (MB) under sunlight [16]. In another study photocatalytic properties of  $\text{Al}_2\text{O}_3$  were explored to degrade Ciprofloxacin in wastewater [17]. Zang *et al.*, investigate the  $\text{AlOOH}$  as photocatalyst for degradation of tetracycline hydrochloride [18].

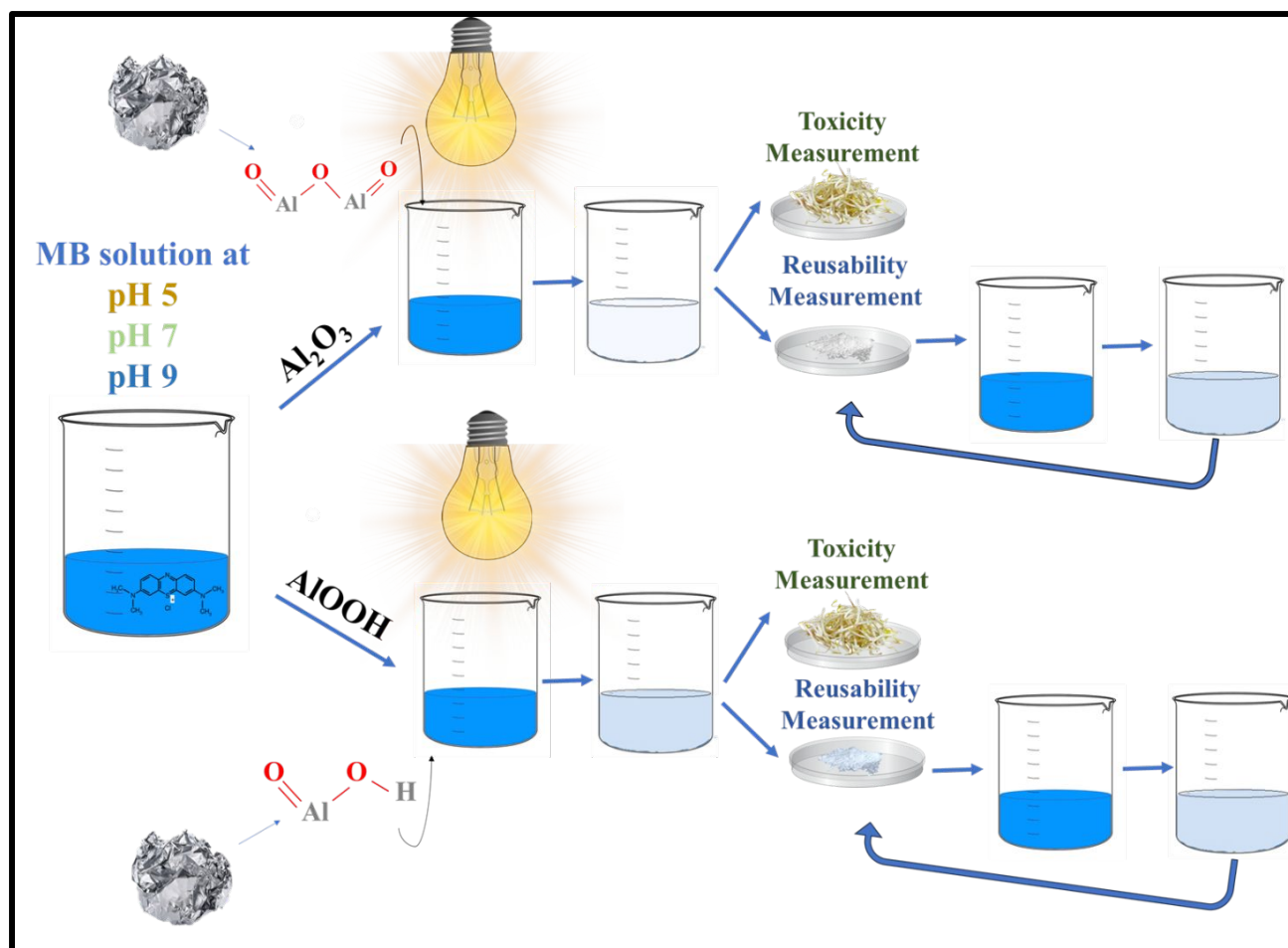
These aluminum particles are significant in continuing to build a sustainable future as population growth and pollution continue to threaten global water supplies. Industrialization further causes a massive influx of dyes and other synthetic chemicals into our waterways; globally, there are about 60,000 tons of waste dye that is released into the environment per year [19,20]. The textile industry is largely responsible for this pollution, however, the removal of dye from wastewater is an incredibly strenuous and expensive process. Methylene blue is a vibrantly colored, cationic dye that is commonly used in many industries such as textile, pharmaceutical, and microbiology (for cell staining) [11,16]. The versatility of this dye lies in its ability to solubilize



in a variety of solvents such as water, ethanol, and acetic acid [16,21]. This dye is very harmful to marine life as well as humans in higher concentrations [21]. Anaerobic reduction, microfiltration, membrane filtration, and other techniques have been employed to try to degrade the MB dye [22-24]. So far, it has been proven that adsorption has been an effective technique for removing the dye from polluted water [22].

Based on the approach of recycling waste to wealth, this research for the first time focuses on the remediation of water containing MB dye by degrading using photocatalytic particles that were prepared from the waste aluminum foil. Synthesized aluminum oxide ( $\text{Al}_2\text{O}_3$ ) and aluminum oxyhydroxide ( $\text{AlOOH}$ ) nanocatalysts were fabricated and characterized using fourier transform infrared spectroscopy (FTIR), Energy-dispersive X-ray spectroscopy (EDX) mapping, X-ray diffraction (XRD), field emission scanning electron microscopy (FE-SEM), UV-vis diffuse reflectance spectroscopy (UV-DRS), and thermogravimetric Analysis/differential scanning calorimetry (TGA/DSC).





**Scheme 1:** Graphical representation of work

These particles were further used for the degradation of cationic MB in neutral basic, and acidic pH medium. Particles were checked for both reusability and toxicity assessment. This research addresses multiple goals simultaneously: reduction in foil solid waste and production of aluminum particles for water pollution removal. Additionally, because the dye is decomposed via visible light, sunlight can be used for the pigment degradation, thus, no additional energy source is required. **Scheme 1** shows the graphical representation of work.

## 2. Experimental details and Procedure:

**2.1. Materials:** Aluminum foil collected from lab waste sites at Panjab University, Chandigarh, Hydrochloric Acid (HCl) and Sodium Hydroxide (NaOH) pellets were procured from ThermoFisher, Sodium carbonate anhydrous LR ( $\text{Na}_2\text{CO}_3$ ) was bought from Rasayan



Laboratories. All chemicals were used in their original state without any later modifications or purification. All experiments were conducted at room temperature in double-distilled water (ddH<sub>2</sub>O). A methylene blue (MB) dye was precured from Sigma-Aldrich. For the toxicity assessment, locally sourced (Chandigarh) mung seeds were used.

## 2.2. Experimental Procedure:

### 2.2.1. Synthesis of Al<sub>2</sub>O<sub>3</sub> and AlOOH:

Waste foil was collected and put in a hot water bath for one hour to remove any earlier contamination. 3.89g foil was then shredded into small, approximately 2-3 cm pieces and added into a 1:1 solution of 23 mL HCl and 23 mL ddH<sub>2</sub>O. This forms an aluminum chloride (AlCl<sub>3</sub>) solution. Once all the foil was completely dissolved into the HCl, the AlCl<sub>3</sub> solution was double filtered into a separate beaker to remove any remaining impurities. This solution was divided into two parts, each half was used to synthesize Al<sub>2</sub>O<sub>3</sub> and AlOOH, respectively.

Al<sub>2</sub>O<sub>3</sub> was synthesized by adding excess Na<sub>2</sub>CO<sub>3</sub> into one of the two halves of the filtered solution until a gelatinous product was formed. This product was transferred into a large beaker washed with excess ddH<sub>2</sub>O, decanted, and washed again. The decantation and washing were repeated twice. The remaining water was disposed of after the second decantation and the solid precipitate was dried in an oven at 45°C for 24 hours and stored in desiccator to remove any moisture content.

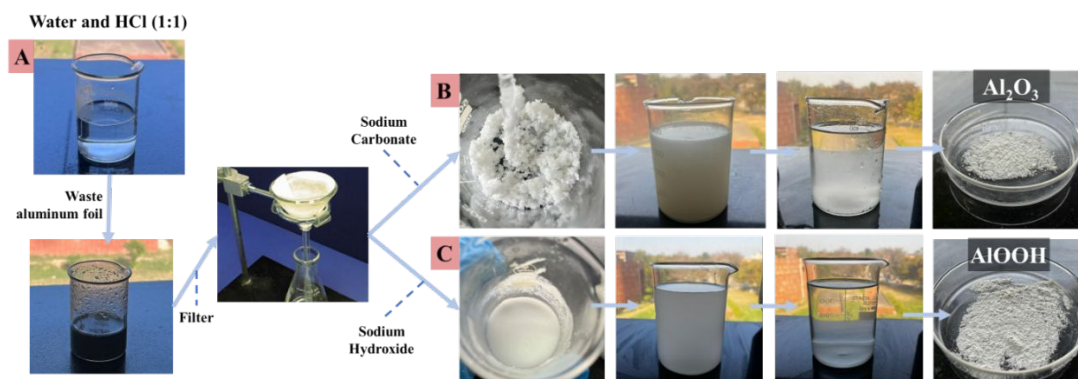


**Figure 1:** Pictures of the synthesis procedure of AlCl<sub>3</sub> (A), Al<sub>2</sub>O<sub>3</sub> (B) and AlOOH (C).

AlOOH was synthesized by adding excess NaOH into the second half of the filtered solution until a gelatinous product formed. This product was transferred into a large beaker



washed with excess ddH<sub>2</sub>O, decanted, and washed again. The decantation and washing were repeated twice. The remaining water was disposed of after the second decantation and the solid precipitate was dried in an oven for at 45° C for 24 hours [25]. **Figure 1** shows the overall step-by-step synthesis procedure from waste aluminum foil.

**2.2.2. Preparation of MB dye:** A 5 ppm MB dye was prepared as a bulk stock solution. The effectiveness of Al<sub>2</sub>O<sub>3</sub> and AlOOH was evaluated under dark and light conditions in a neutral pH of 7, basic pH of 9, and acidic pH of 5. Basic pH conditions were created by the addition of NaOH pellets to a part of the bulk solution and acidic pH conditions were created by adding HCl to a part of the bulk solution. The pH of the solution after the addition of NaOH and HCl was measured by a pH meter (Labman Scientific Instrument).

**2.2.3. Characterization:** Several instruments were employed to analyze the synthesized Al<sub>2</sub>O<sub>3</sub> and AlOOH particles. Chemical bonds in the samples were characterized using Perkin Elmer Spectrum II FTIR with a scanning range of 4000 cm<sup>-1</sup> to 400 cm<sup>-1</sup>. The morphology, topology, and metallographic details of the particles were observed using a Field Emission – Scanning Electron Microscope (FE-SEM) of the HITACHI SU8010 series. Solid material was casted on carbon tape and coated with a gold sputter coating machine for 15 mA for 20 seconds. For mapping and EDX analysis, the operating voltage was 15 kV and the working distance was 15 mm. The elemental analysis was performed using EDS-Bruker SDD XFlash 6130. An Anton Parr Litesizer 500 Zeta-sizer was used to measure the particle size and zeta-potential (mV). The DLS experiments were performed on the instrument equipped with a front scattered angle of 15°, a side scattered angle of 90°, a back scattering angle of 173°, and a He-Ne laser (wavelength = 633 nm, power = 4 mW). The thermal properties of the prepared particles were investigated by thermo-gravimetric analysis (TGA-DTA) on the SDT Q-600 instrument. The crystallographic structure was explored using an X'Pert Pro X-Ray Diffraction (XRD) spectrophotometer. UV-vis diffuse reflectance spectroscopy (UV-DRS) (Jasco V-750) was used to calculate the band gaps of Al<sub>2</sub>O<sub>3</sub> and AlOOH.

**2.2.4. Photocatalytic Activity Experiments:** Total 25 ml of the dye stock at 5 PPM was used along with 50 mg of each particle for all experiments. The solutions with the photocatalysts were placed under dark and visible light conditions at pH 7, pH 9, and pH 5, for two trials each. A visible light





bulb (500 W tungsten lamp) was used for this experiment was placed approximately 12 inches above the beaker (containing the MB contaminated water and photocatalyst particles). The absorbance of each solution was recorded in 30-minute intervals for 240 minutes by UV-Vis spectrophotometer (LABINDIA UV 3200). A quartz cuvette was used for the measurement. The following equation was used to calculate the degradation efficiency (DE) of the particles in the dye:

$$DE (\%) = \frac{C_t}{C_0} (100) \quad (1)$$

Where DE is Degradation Efficiency in percent,  $C_0$  is the first concentration and  $C_t$  is the final concentration of dye after time 't' of photodegradation.

Further methylene blue intermediates' formation after photocatalytic degradation were analysed with a mass spectrometer (Waters Corporation, U.K, Model: Alliance 2795, Q-TOF Micromass Mass spectrometer).

**2.2.5. Toxicity Study:** The growth of locally sourced mung seeds (*Vigna radiata*) was measured in four conditions: control (ddH<sub>2</sub>O), untreated dye water (5 ppm), treated Al<sub>2</sub>O<sub>3</sub> water, and treated AlOOH water. A total of 250 mL dye solution (MB 5ppm) was prepared in bulk. It should also be noted that Al<sub>2</sub>O<sub>3</sub> and AlOOH were used to degrade 250 mL of 5 ppm MB each producing 250 mL of water treated by Al<sub>2</sub>O<sub>3</sub> and 250 ml of water treated by AlOOH. The water that was treated in bulk was used for this toxicity assessment. 10 seeds were placed in each petri dish and 15 mL of the respective solution was added daily. The Petri dishes were placed in a dark area and observed for 14 days.

The following equation was used to determine the Germination Index ( $G_i$ ):

$$G_i = \frac{G}{G_0} * \frac{L}{L_0} (100) \quad (2)$$

Where G and L are germinations and root length in the treated solution and  $G_0$  and  $L_0$  are germinations and root length in 100% ddH<sub>2</sub>O control solution [26].



**2.2.6. Reusability Study:** The reusability of both particles was evaluated in three main cycles in neutral pH, under visible light conditions. In the first cycle, after the initial degradation of MB, the particles were retrieved and dried. These particles were then measured out again and a degradation cycle was initiated. The quantities of the particles and solution were kept consistent with 50 mg particles in 25 mL solution.

### 3. Result and discussion:

#### *Synthesis and characterizations:*

FTIR and XRD were used to characterize the prepared particles. **Figure 2(a)** represents the contrast between the FTIR spectrum of the synthesized  $\text{Al}_2\text{O}_3$  (black) and  $\text{AlOOH}$  (red). Both samples showed peaks in the fingerprint region that can be attributed to the bending and stretching vibrations, which are characteristics shared amongst organic compounds. Impurities in the waste aluminum foil that was used for the synthesis can be blamed for the organic compounds [27]. Peaks seen at  $\text{Al}_2\text{O}_3$  at 482, 532, 952, and  $1385\text{cm}^{-1}$  are the bending and stretching of the Al-O interactions [27,28]. For  $\text{AlOOH}$ , these peaks were seen at 481, 581, 713, 973, and  $1395\text{cm}^{-1}$ . In addition to representing the Al-O interactions, peaks at lower wavelengths also signify a pseudo-boehmite structure. Specifically, this incomplete crystalline boehmite structure is seen in both molecules and contains aluminum-based matrix materials [29,30]. A band in  $\text{Al}_2\text{O}_3$  is also observed at  $656\text{cm}^{-1}$  which is correlated to the Al-O-Al interactions within the molecule [27]. The peaks in  $\text{Al}_2\text{O}_3$  at  $1556\text{cm}^{-1}$  and in  $\text{AlOOH}$  at  $1668\text{cm}^{-1}$  can be attributed to a cis-double bond in the molecule [27]. Bands are also seen at  $726\text{cm}^{-1}$ , which correlated to the tetrahedral structures found in  $\text{Al}_2\text{O}_3$  [26]. The broad peaks seen in both samples around  $3302\text{cm}^{-1}$  ( $\text{Al}_2\text{O}_3$ ) and  $3423$  ( $\text{AlOOH}$ ) represent the vibrating of the Al-O-H bonds in the sample [31].

XRD is used to interpret the structures of atoms found inside a sample and can dictate whether a sample is crystalline or amorphous. The XRD results in **Figure 2(b)** were produced by  $\text{Al}_2\text{O}_3$  and  $\text{AlOOH}$ . For  $\text{Al}_2\text{O}_3$  peaks were observed at  $2\theta = 13.17^\circ, 18.84^\circ, 20.33^\circ, 27.95^\circ, 33.13^\circ, 40.66^\circ, 49.24^\circ, 53.33^\circ, 63.99^\circ, \text{ and } 70.98^\circ$ . These results were comparable with XRD results for pure  $\text{Al}_2\text{O}_3$  given in the JCPDS [32]. It can be inferred that peaks  $2\theta = 27.95^\circ, 49.24^\circ, 53.33^\circ, \text{ and}$



63.99° are caused by the presence of NaCl. These NaCl peaks are further confirmed in the literature [33]. It can also be inferred that the peaks at  $2\theta = 27.95^\circ$ ,  $40.66^\circ$ ,  $49.24^\circ$ , and  $70.98^\circ$  are caused by the presence of  $\text{Al}_2\text{O}_3$ . A sharp peak insinuates that the cell arrangement of the sample is crystalline [32,34]. Peaks for AIOOH were observed at  $2\theta = 15.35^\circ$ ,  $32.27^\circ$ ,  $43.23^\circ$ , and  $53.99^\circ$ . Saravanan, et al. (2023) found the XRD pattern for AIOOH at  $2\theta = 27.4^\circ$ ,  $38.3^\circ$ ,  $48.8^\circ$  and  $64.9^\circ$  [25,35]. The broad width of the peak suggests that AIOOH consists of nanocrystals, however, the peaks are not sharp suggesting that the molecule consists of an orthorhombic structure [25,36]. The peaks observed in the AIOOH are in correspondence with the literature but some negative shift in the  $2\theta$  was found. This may be due to the NaCl present in the sample.

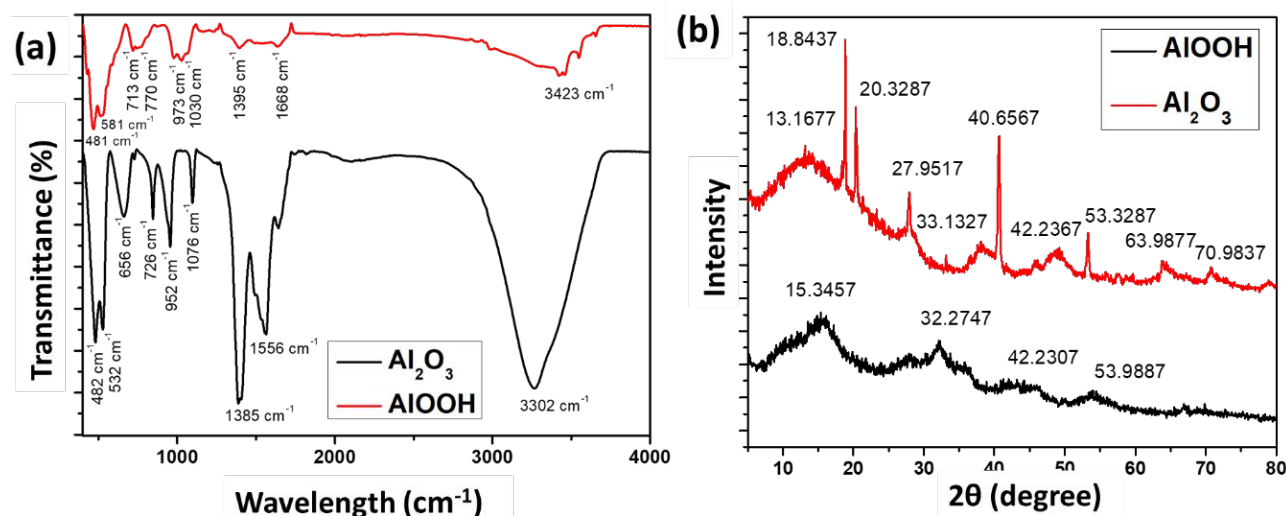


**Figure 2:** FTIR (a) of  $\text{Al}_2\text{O}_3$  (black) and AIOOH (red). XRD (b) of  $\text{Al}_2\text{O}_3$  (red) and AIOOH (black).

The absorbances of  $\text{Al}_2\text{O}_3$  (10mg in 2 mL) and AIOOH (10mg in 2 mL) in water were also recorded using UV-Vis spectrophotometry as seen in **Figure S1**. It was observed that the absorption peak of  $\text{Al}_2\text{O}_3$  and AIOOH in ddH<sub>2</sub>O matches the literature results [37,38]. The band gap of the  $\text{Al}_2\text{O}_3$  and AIOOH samples have been calculated by performing UV-vis DRS study. In literature, it is reported that band gap changes with crystalline nature of  $\text{Al}_2\text{O}_3$  and also can be modulated when combined with other materials, however, if the calcination process is not complete, the surface hydroxyl groups can reduce the band gap, allowing it to act as a photocatalyst [39-41]. Edalati *et al.*, reduced the  $\text{Al}_2\text{O}_3$  band gap to below 3eV by high pressure torsion (HPT) method [42].



Kusuma *et al.*, explored the photocatalytic properties of Al<sub>2</sub>O<sub>3</sub> where Al<sub>2</sub>O<sub>3</sub> nanoparticles exhibited an energy band gap of 4.46 eV; these particles were used for MB degradation [43]. Additionally, Nduni *et al.*, reported that Al<sub>2</sub>O<sub>3</sub> particles prepared using green approach from waste aluminium foil have band gap of 5.25 eV [27]. It is evident that both Al<sub>2</sub>O<sub>3</sub> and AlOOH can degrade dye in the presence of light; however, they are unable to perform this function in the dark. This suggests that these compounds can act as photocatalysts. To further support these findings, the band gap energy was determined using a Tauc plot. [38]. **Figure S2** depicts  $(\alpha h\nu)^2$  vs. Energy (eV) of Al<sub>2</sub>O<sub>3</sub> and AlOOH. It was determined that Al<sub>2</sub>O<sub>3</sub> has a band gap of 4.29 eV and AlOOH has a band gap of 5.50 eV. The band gap of Al<sub>2</sub>O<sub>3</sub> at 4.29 eV proves that this particle possibly has photocatalytic nature.

The TGA results for Al<sub>2</sub>O<sub>3</sub> and AlOOH are seen in **Figure S3(a&b)**. A multi-step decomposition for both particles is observed. In Al<sub>2</sub>O<sub>3</sub> (**Figure S3(a)**) there is a 38.16% (2.15 mg) initial loss in weight (up to 100°C), indicating dehydration. Then, there is a 20.13% loss in mass (1.14 mg) around 300°C indicating decomposition. The decomposition that has occurred at this temperature matched the results observed by Gondal *et al.* [44]. In total, there was about a 70.97% loss in mass when the temperature reached 900°C. AlOOH (**Figure S3(b)**) also follows a similar multistep decomposition. Initially, 22.29% of the total mass was lost between 50-100°C, suggesting dehydration. Then, around 250-300°C, there was an 11.77% mass loss due to decomposition. There was a 52.633% mass loss when the temperature reached 900°C.

The heat flow in the Al<sub>2</sub>O<sub>3</sub> sample is detected by the DSC measurement. Endothermic dips are seen at 100°C and 300°C, which is the same temperature range at which decomposition occurred. This implies that the sample is melting at these temperatures. DSC peaks are seen at 200°C and 700°C suggesting some crystallization in the sample. The heat flow in the AlOOH sample is also detected by the DSC measurement. Endothermic dips are seen around 50 - 100°C and 250- 300°C, which is the same temperature range at which decomposition occurred. This implies that the sample is melting at these temperatures. A DSC peak is seen at 275°C revealing some crystallization in the sample.

FE-SEM results in **Figure 3** confirm the surface morphology of the particles. It was observed that Al<sub>2</sub>O<sub>3</sub> has a jagged and rough surface, that consists of different size pores, as seen



in **Figure 3(a&b)**. The surface of this particle is more heterogeneous and larger than the AlOOH particle. The AlOOH particle has a much smaller surface area, compared to Al<sub>2</sub>O<sub>3</sub> (**Figure 3(c&d)**). These nanoparticles also contain various-sized cavities and pores, making the particle look slightly rugged.

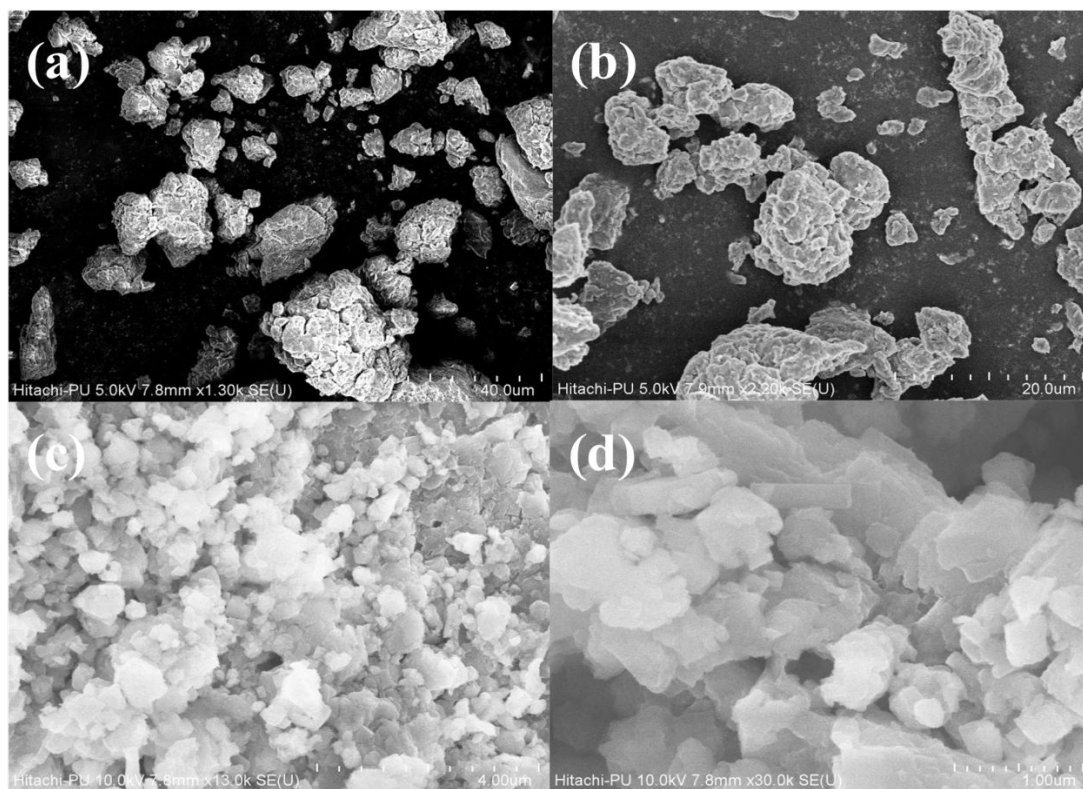


**Figure 3:** FE-SEM of Al<sub>2</sub>O<sub>3</sub> (**a, b**) particles at scale 40.0 μm and 20.0 μm (respectively). FESEM of AlOOH (**c, d**) particles at scale 4.0 μm and 1.0 μm (respectively).

The results for mapping and EDX of Al<sub>2</sub>O<sub>3</sub> and AlOOH are presented in **Figure 4**. The elements that were observed in the mapping of Al<sub>2</sub>O<sub>3</sub> consist of mainly Al and O atoms (**Figure 4 (a-c)**). There is a smaller amount of Na and Cl atoms, which can be attributed to the HCl in the synthesis of the particles (**Figure 4(d)**). These can be constituted as impurities in the sample. The elements that were observed in the mapping and EDX of AlOOH also mainly consist of Al and O with a much smaller amount of Cl and Na (**Figure 4 (e-h)**). Overall, the mapping verifies that Al and O atoms are distributed homogeneously on the surface of both particles. The gold (Au) present in the EDX mapping is due to the Au coating that was applied to the Al<sub>2</sub>O<sub>3</sub> and AlOOH during the FESEM process.



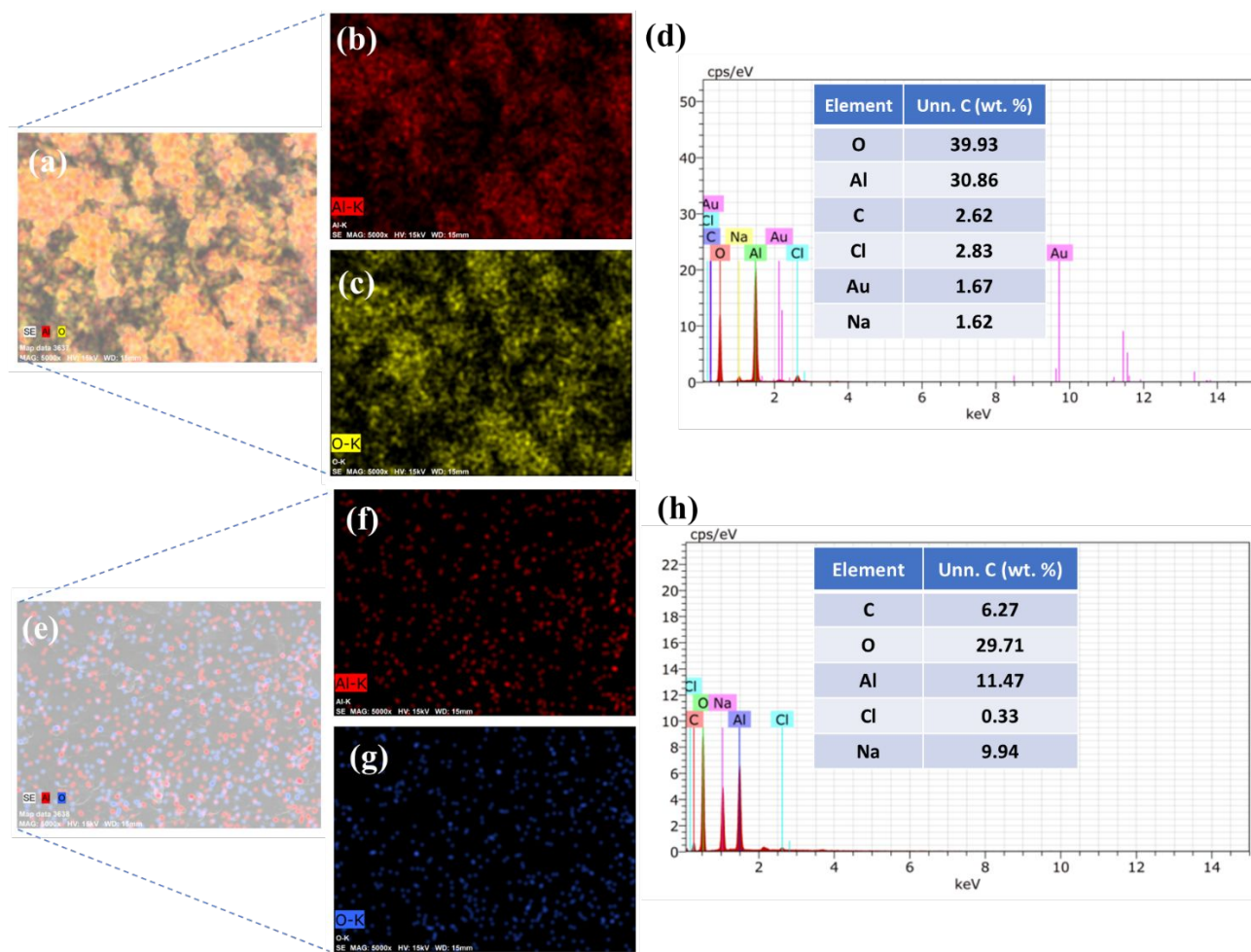


**Figure 4:** Mapping of Al<sub>2</sub>O<sub>3</sub> (a,b,c) and EDX of Al<sub>2</sub>O<sub>3</sub> (d). Mapping of AlOOH (e, f, g) and EDX of AlOOH (h).

The zeta-size results are presented in **Table 1** and **Figure S4-S6**. The hydrodynamic diameter and polydispersity index of the synthesized Al<sub>2</sub>O<sub>3</sub> and AlOOH were calculated at pH 5, 7 and 9. This study shows that at pH 5 Al<sub>2</sub>O<sub>3</sub> particles have hydrodynamic diameters around 3257 nm and then it decreases with pH change to 1133 nm and 856.9 nm at pH 7 and 9, respectively. For AlOOH particles hydrodynamic diameter change with change in pH value. Overall PDI value of the for both Al<sub>2</sub>O<sub>3</sub> and AlOOH particles are still less than 52%. Zeta-potential values for Al<sub>2</sub>O<sub>3</sub> was 11 mV at 5 pH and then by changing pH to 7 and 9 zeta-potential changed to -15.7 mV and -26.9 mV,



respectively. At pH 5 for AlOOH zeta-potential was -20.7 mV and change to 4.3 mV and -17.0 mV at pH to 7 and 9, respectively.

**Table 1:** Hydrodynamic diameter, polydispersity index, and zeta-potential of Al<sub>2</sub>O<sub>3</sub> and AlOOH.

pH	Sample	Hydrodynamic Diameter (D <sub>h</sub> ) in nm	Polydispersity Index (PDI)	Zeta-potential (mV)
5	Al <sub>2</sub> O <sub>3</sub>	3257	47.8%	11
	AlOOH	1803.4	37.0%	-20.7
7	Al <sub>2</sub> O <sub>3</sub>	1133	52.6%	-15.7
	AlOOH	3513	38.9%	4.3
9	Al <sub>2</sub> O <sub>3</sub>	856.9	31.4%	-26.9
	AlOOH	806.5	8.8%	-17.0

#### *Degradation of Dye Under pH 7, pH 9, and pH 5:*

**Figure 5** shows a comprehensive analysis of the degradation of MB in different conditions using Al<sub>2</sub>O<sub>3</sub> and AlOOH as catalysts, both in the dark and under visible light at pH 7. **Figure 5(a)** depicts the MB solution with Al<sub>2</sub>O<sub>3</sub> in the dark observed for 240 minutes. This reaction was performed at pH 7. Initially, the concentration of the solution decreased, followed by stabilization. **Figure 5(b)** depicts the MB solution with AlOOH in the dark observed for 240 minutes at pH 7. Like Al<sub>2</sub>O<sub>3</sub>, the concentration of the solution initially decreases and then stabilizes.



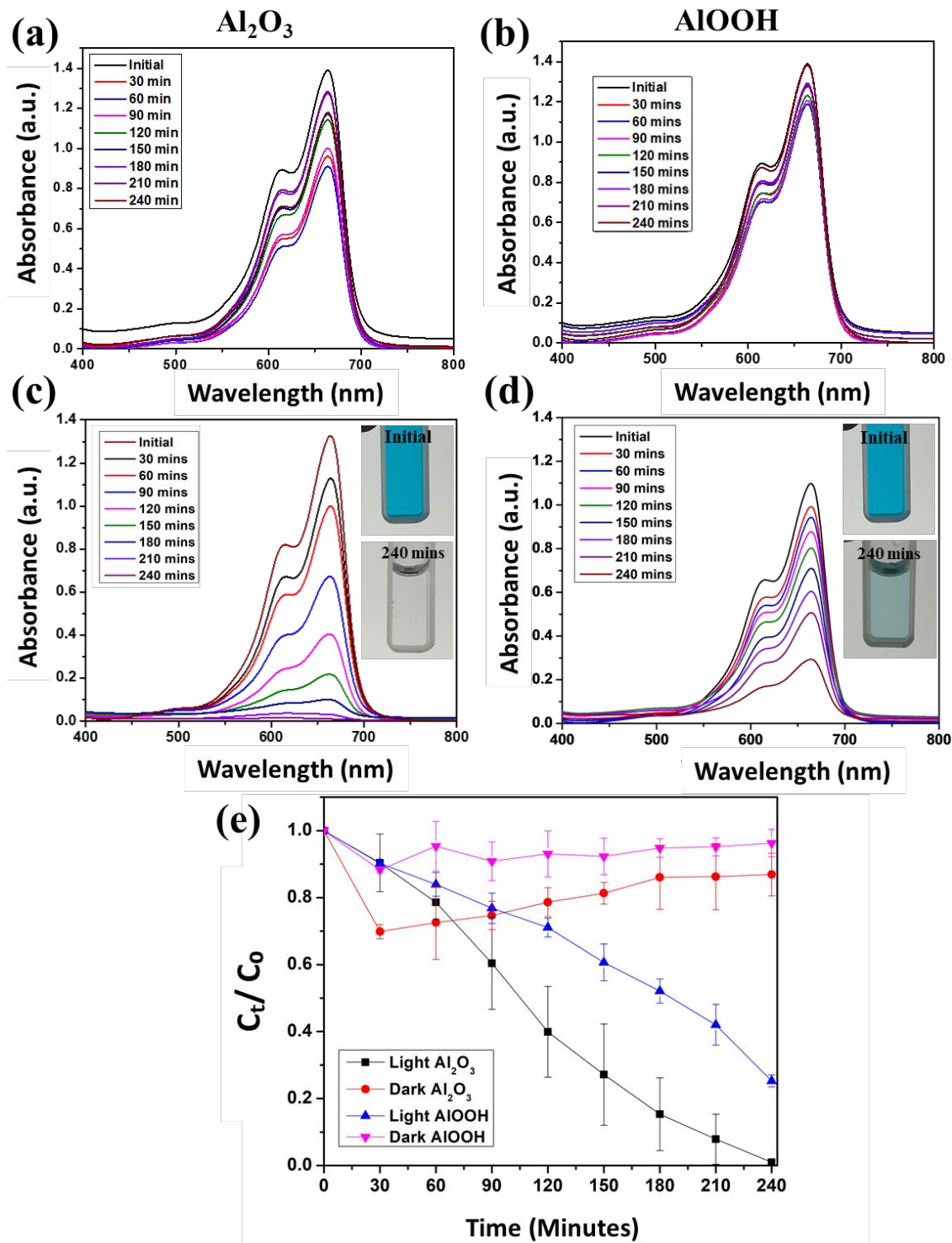


**Figure 5:** UV-Vis spectra of MB with  $\text{Al}_2\text{O}_3$  (a),  $\text{AlOOH}$  (b) in the dark and  $\text{Al}_2\text{O}_3$  (c),  $\text{AlOOH}$  (d) in the light at pH 7. Average degradation efficiency over time at pH 7 (e).

The concentration decrease range was significantly greater with  $\text{Al}_2\text{O}_3$  compared to  $\text{AlOOH}$  in the absence of light, which also signifies the adsorption of dye on particles in the dark.





**Figure 5(c)** depicts the MB solution with  $\text{Al}_2\text{O}_3$  in visible light observed for 240 minutes at pH 7. The concentration of the solution steadily decreased for 240 minutes and eventually became clear. This demonstrates photocatalytic degradation of MB under visible light by  $\text{Al}_2\text{O}_3$ . **Figure 5(d)** depicts the MB solution with  $\text{AlOOH}$  in visible light observed for 240 minutes, at pH 7. The concentration of the solution steadily decreased for 240 minutes. **Figure 5(e)** shows the time-dependent concentration decrease in the dye degradation with irradiation time.

When the reactions were performed in the dark, in neutral pH conditions, there was a 17.60% and 6.64% degradation in the MB solution with  $\text{Al}_2\text{O}_3$  and  $\text{AlOOH}$  in the absence of light. When the reactions were performed in visible light, under neutral conditions, there was a 99.29% degradation in the MB solution with  $\text{Al}_2\text{O}_3$ , and 75.98% degradation in the MB solution with  $\text{AlOOH}$  was observed. In dark conditions, the concentration was seen dropping initially, within the first 30-60 minutes, then slowly becoming constant. This can be attributed to the first adsorption of the MB into the particles, which was then released back into the solution, causing the concentration to slightly fluctuate. The degradation efficiency of MB ( $C_t/C_0$ ) vs. time is also seen in **Figure 5(e)**, which is the average of both, trial 1 and trial 2. This indicates that  $\text{AlOOH}$  also facilitates photocatalytic degradation of MB under visible light, though possibly less efficiently than  $\text{Al}_2\text{O}_3$ . Then same experiment was performed at pH 9 and accordingly **Figure 6(a)** represents the MB solution with  $\text{Al}_2\text{O}_3$  in the dark observed for 240 minutes. The concentration of the solution drastically decreased for 60 minutes and then stabilized with some inconsistencies. **Figure 6(b)** shows the MB solution with  $\text{AlOOH}$  in the dark observed for 240 minutes at pH 9. The concentration of the solution drastically decreased for 90 minutes, after which it again became stable with slight oscillation.



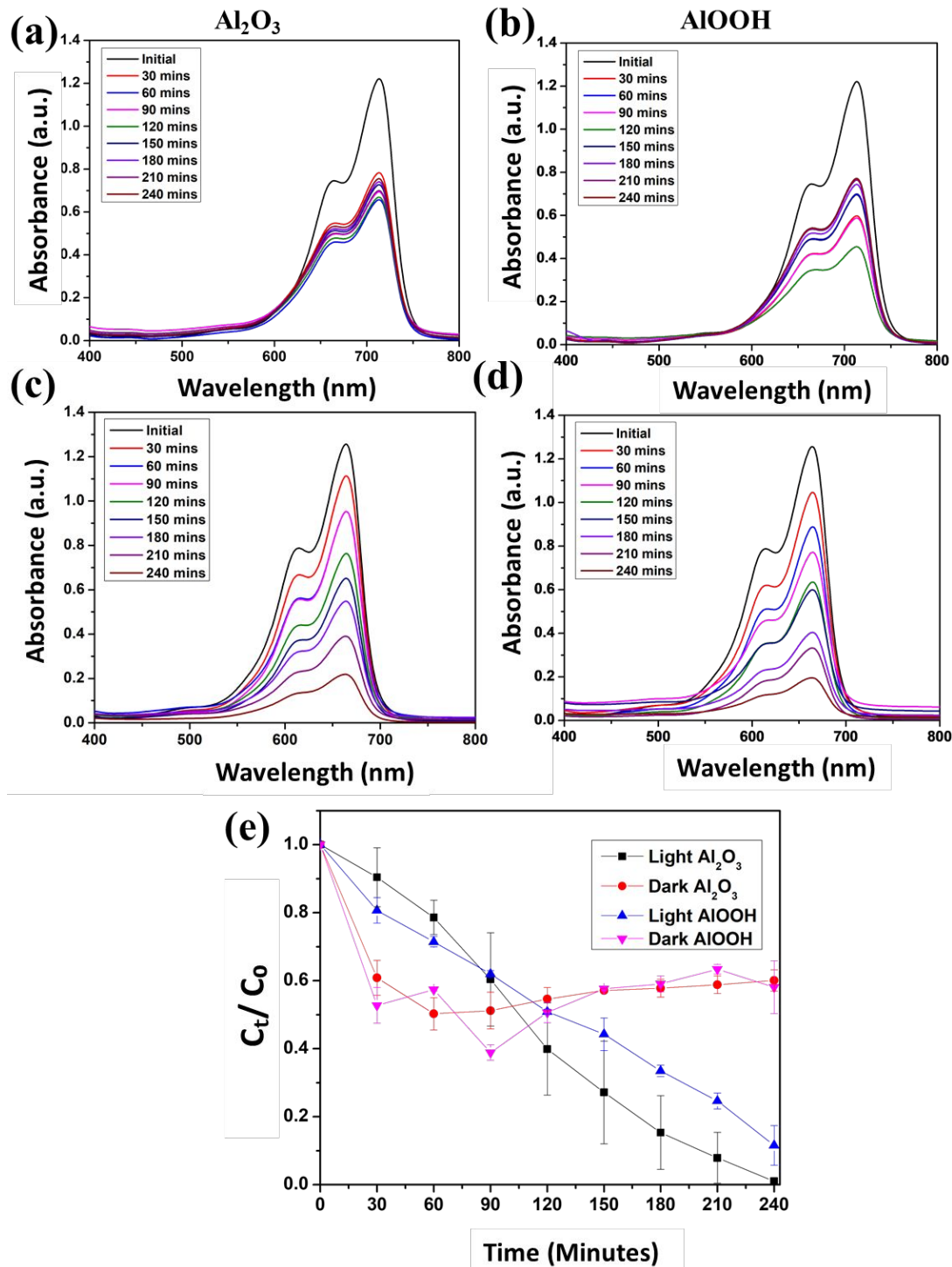


**Figure 6** UV-Vis spectra of MB with  $\text{Al}_2\text{O}_3$  (a),  $\text{AlOOH}$  (b) in the dark and  $\text{Al}_2\text{O}_3$  (c),  $\text{AlOOH}$  (d) in the light at pH 9. Average degradation efficiency over time at pH 9 (e).

**Figure 6(c)** depicts the MB solution with  $\text{Al}_2\text{O}_3$  in visible light was observed for 240 minutes at pH 9. The concentration of the solution consistently decreased for 240 minutes, till it reached 0.21



a.u. **Figure 6(d)** represents the MB solution with AlOOH in visible light observed for 240 minutes at pH 9. The concentration of the solution consistently decreased for 240 minutes, till it reached 0.18 a.u.

When the reactions were performed in the dark, under basic conditions, there was a 37.88% degradation in the MB solution with Al<sub>2</sub>O<sub>3</sub>. There was a 37.70% degradation in the MB solution with AlOOH. Despite having similar degradation efficiencies, AlOOH initially absorbed MB more effectively than Al<sub>2</sub>O<sub>3</sub> under basic conditions in the dark. There was a larger range of absorbance in AlOOH than in Al<sub>2</sub>O<sub>3</sub> in the dark. When the reactions were performed in visible light, under basic conditions, there was an 82.77% degradation in the MB solution with Al<sub>2</sub>O<sub>3</sub> and an 84.58% degradation in the MB solution with AlOOH. In the dark conditions, the concentration was seen drastically dropping within 60-90 minutes, before showing slight inconsistencies with slight upwards and downwards variation. The degradation efficiency of MB vs. time is also seen in **Figure 6(e)**, which is the average of two trials. It was observed that in basic conditions in the dark, AlOOH adsorbs MB more effectively than Al<sub>2</sub>O<sub>3</sub>. After the initial concentration change of MB, the concentrations of both solutions stabilize with slight variations.

Another experiment was conducted to evaluate the photocatalytic efficiency of catalyst under acidic condition. This reaction was performed at pH 5. **Figure 7(a&b)** represents the MB solution with Al<sub>2</sub>O<sub>3</sub> and AlOOH in the dark observed for 240 minutes, respectively. The concentration of the dye decreased for 30-60 minutes and overall, the concentration of MB remained consistent for the 240 minutes. **Figure 7(c)** and **Figure 7(d)** depicts the MB solution with Al<sub>2</sub>O<sub>3</sub> and AlOOH in visible light observed for 240 minutes, respectively. With both particles the concentration of the MB consistently decreased for 240 minutes, till it reached a clear solution.



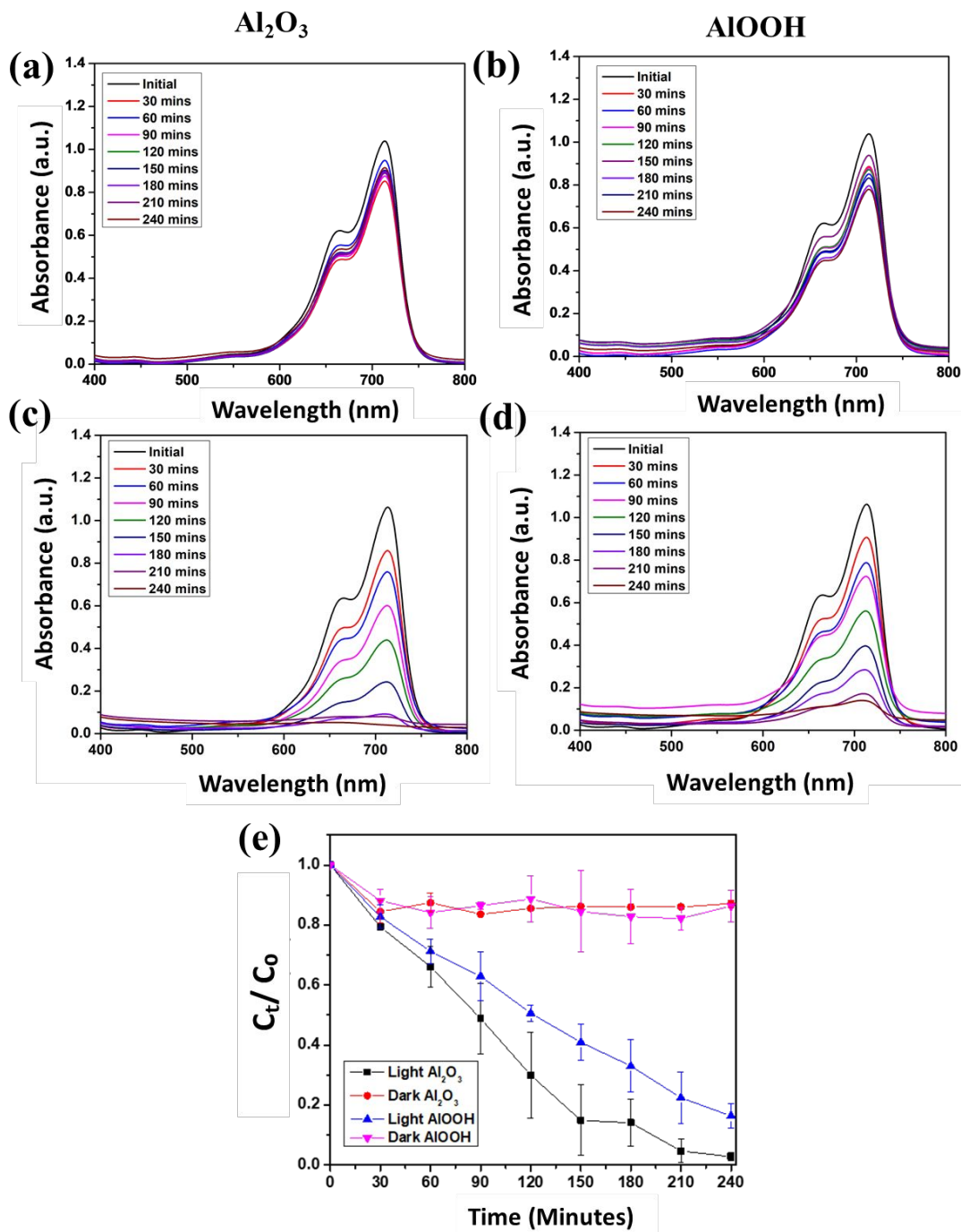


**Figure 7:** UV-Vis spectra of MB with  $\text{Al}_2\text{O}_3$ (a),  $\text{AlOOH}$ (b) in the dark and  $\text{Al}_2\text{O}_3$ (c),  $\text{AlOOH}$ (d) in the light at pH 5. Average degradation efficiency over time at pH 5(e).

When the reactions were performed in the dark, under acidic conditions, there was a 12.34% degradation in the MB solution with  $\text{Al}_2\text{O}_3$  was observed. There was a 33.22% degradation



in the MB solution with AlOOH. AlOOH and Al<sub>2</sub>O<sub>3</sub> were equally effective at adsorbing MB in the dark. When this reaction was performed in visible light, there was a 97.88% degradation in the MB solution with Al<sub>2</sub>O<sub>3</sub> and an 86.67% degradation in the MB solution with AlOOH. The dye was consistently degraded in visible light with both Al<sub>2</sub>O<sub>3</sub> and AlOOH. The graph in **Figure 7(e)** depicts the average of two trials that were performed during the degradation reactions of MB. It is observed that Al<sub>2</sub>O<sub>3</sub> and AlOOH shows similar patterns in acidic conditions. Under light, both Al<sub>2</sub>O<sub>3</sub> and AlOOH are consistently decreasing, however, Al<sub>2</sub>O<sub>3</sub> is still more effective than AlOOH.

Overall, it can be observed that the MB solution was degraded the most efficiently in neutral conditions under visible light with Al<sub>2</sub>O<sub>3</sub>; MB was degraded the least efficiently in neutral conditions under the dark with AlOOH(**Table 2**). The range between the highest and lowest degradation efficiency under all conditions is 92.65%. Specifically, in neutral conditions, Al<sub>2</sub>O<sub>3</sub> performed better than AlOOH in the dark and the light. There was significantly more degradation in the light than in the dark. This proves that the dye is primarily adsorbed in the dark but degraded in the light. Al<sub>2</sub>O<sub>3</sub> and AlOOH both performed better in the dark after the pH was increased from neutral to alkaline (7 to 9). In the light at pH 9, however, the efficiency of Al<sub>2</sub>O<sub>3</sub> decreased while the efficiency of AlOOH increased by 8.59%. At pH 9, AlOOH is proven to be a more effective photocatalyst than when used at pH 7. In the dark at pH 5, AlOOH was significantly more effective (20.88% more effective) at degrading MB when compared to Al<sub>2</sub>O<sub>3</sub>. However, in the light under acidic conditions, Al<sub>2</sub>O<sub>3</sub> was 11.21% more effective than AlOOH at degrading MB.

Overall, when only the dark conditions are considered at all pH's, it was observed that Al<sub>2</sub>O<sub>3</sub> is least effective at pH 5 and most effective at pH 9 and AlOOH is least effective at pH 7 and most effective at pH 9. The range between the highest and lowest degradation efficiency in the dark under all pH's is 31.24%. When only visible light conditions are considered at all pH's, it is observed that Al<sub>2</sub>O<sub>3</sub> is consistently more effective than AlOOH for the photocatalytic degradation of MB. At pH 7, Al<sub>2</sub>O<sub>3</sub> is the most effective while AlOOH is the least effective. Nevertheless, it was discovered that the efficiency of AlOOH was improved by increasing and decreasing the pH. The range between the highest and lowest degradation efficiency in visible light under all pH's is 23.30%(**Table 2**).



In order to determine the kinetics of dye degradation, the first-order kinetic was applied  $\ln(C_t/C_0) = -kt$ , where,  $C_t$  and  $C_0$  are the final concentration that particular point of time (min) and initial concentrations of the MB dye, respectively and  $k$  is the rate constant. Figure S7-S9 depicts  $\ln(C_t/C_0)$  vs time (min) intervals plot shows the linear correlation was obtained by plotting for the degradation of MB, suggested that the removal of MB dye using  $\text{Al}_2\text{O}_3$  and  $\text{AlOOH}$  followed pseudo-first-order kinetics.

**Table 2:** Comparison between the degradation efficiencies at pH 7, pH 9, and pH 5 in dark and visible light conditions

	pH 5		pH 7		pH 9	
	$\text{Al}_2\text{O}_3$	$\text{AlOOH}$	$\text{Al}_2\text{O}_3$	$\text{AlOOH}$	$\text{Al}_2\text{O}_3$	$\text{AlOOH}$
<b>Dark</b>	12.34%	33.22%	17.60%	6.64%	37.88%	37.70%
<b>Light</b>	97.88%	86.67%	99.29%	75.99%	82.77%	84.58%

**Figure 8(a-e)** illustrates the behavior of the MB solution in both darkness and light, with and without photocatalysts. Initially, the MB solution is shown in **Figure 8(a)**. After 240 minutes of light exposure, the solution becomes colorless in the presence of  $\text{Al}_2\text{O}_3$  and  $\text{AlOOH}$  (**Figures 8(b)** and **8(c)**). Conversely, under dark conditions, the solution remains colored with  $\text{Al}_2\text{O}_3$  and  $\text{AlOOH}$  (**Figures 8(d)** and **8(e)**). This picture clearly showed the effect of catalyst in absence and presence of light which also confirmed that in presence of light photodegradation occurred.

Further to check the intermediate formation after effective photocatalytic active of  $\text{Al}_2\text{O}_3$  aliquid chromatography-mass spectrometry (LC-MS) test was performed on the initial MB, MB with  $\text{Al}_2\text{O}_3$  in the dark and the MB with  $\text{Al}_2\text{O}_3$  under light after 240 mins. **Figure 8(f-h)** shows the full range mass scan graph of pure MB without treatment, MB with  $\text{Al}_2\text{O}_3$  under dark and presence of light, respectively. Pure and MB with  $\text{Al}_2\text{O}_3$  in the dark condition showed very similar



results with peaks seen approximately at 270, 284 (largest peak), 285 and 286 m/z. The maximum percentage peak at m/z=284 corresponds to the M<sup>+</sup> molecular ion of methylene blue that matches the reported literature value of MB base peak value [45]. The identical results in both (Pure and MB with Al<sub>2</sub>O<sub>3</sub> in the dark condition) further showed that there was no photocatalytic intermediate product were formed. On the otherhand, when the experiment was performed in the light, the following peaks were observed: 72.93, 72.98, 88.98, 89.9, 96.96, 97.96, 112.95, 116.97, 130.00, 138.95, 158.00, 166.95, 179.98, 202.17, 207.98, 224.12, 241.92, 254.92, 267.94, 281.89 m/z and about 14 more distinguishable peaks. The number of peaks significantly increasing show that there was a formation of new products caused by the photodegradation of the original MB with Al<sub>2</sub>O<sub>3</sub>. Peaks seen at different m/z are consistent with the possible mass spectra obtained for MB after degradation[45](**Figure 8**).

The presence of only three peaks in the initial LC-MS graphs represents the primary molecular components of the sample. The lack of change in this sample after allowing the catalyst to interact with the MB in the dark for 240 mins suggests that the parent compound has not changed. However, when the sample was tested after exposure to light for 240 mins, where was the appearance of different peak suggests that the original molecules have likely fragmented into smaller pieces, each with a different mass-to-charge ratio, leading to new peaks [45-46](**Figure 8**).

To further prove the photodegradation process of Al<sub>2</sub>O<sub>3</sub>, an experiment was also performed at higher concentration of MB i.e., 20 ppm. The results of the experiment in the dark and in the light are presented in Fig. S10. The results show that MB continues to degrade under light with Al<sub>2</sub>O<sub>3</sub>.



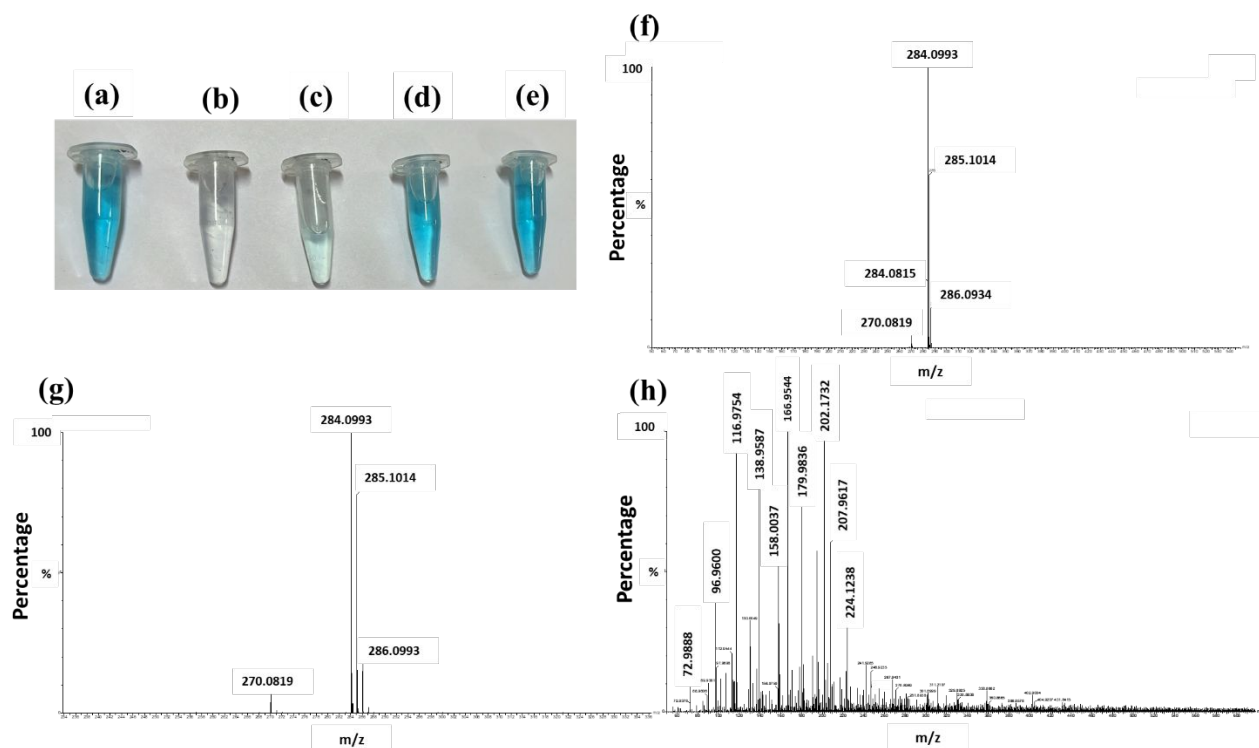


**Figure 8:** Samples of the MB **(a)** Initial, **(b)** with  $\text{Al}_2\text{O}_3$  in the light after 240 mins, **(c)** with  $\text{AlOOH}$  in the light after 240 mins, **(d)** with  $\text{Al}_2\text{O}_3$  in the dark after 240 mins, and **(e)** with  $\text{AlOOH}$  in the dark 240 mins. Mass spectra of MB **(f)** Initial, **(g)** 240 mins in the Dark, and **(h)** 240 mins in the Light.

For the toxicity analysis, the mung seeds were incubated at room temperature for 14 days in the dark [47]. After incubation, the number of seeds that germinated (G) and the root length (L) were measured for seeds in each condition: ddH<sub>2</sub>O, 5 PPM MB, treated  $\text{Al}_2\text{O}_3$  water, and treated  $\text{AlOOH}$  water. The MB solution was treated (under visible light) with  $\text{Al}_2\text{O}_3$  and  $\text{AlOOH}$  in water in bulk reactions proving that these particles can operate in larger-scale reactions.





**Table 3:** Number of seeds germinated and their respective lengths, used to calculate  $G_i$  and the Germination index ( $G_i$ ) of mung seeds in control, MB,  $Al_2O_3$  and AIOOH

Sample	#G	L (cm)	$G_i$
Control	18	76.25	100
MB	14	36.75	37.48634
$Al_2O_3$	18	34	44.59016
AIOOH	15	25.251	27.59563

The results of the toxicity assessment concluded that ddH<sub>2</sub>O produced the most germinated seeds followed by  $Al_2O_3$ , AIOOH, and MB, respectively (**Table 3**) (**Figure 9**). However, despite having more germinated seeds, the germination index for AIOOH was lower than the one of MB as the seeds in MB solution grew longer. This increased the overall germination index.

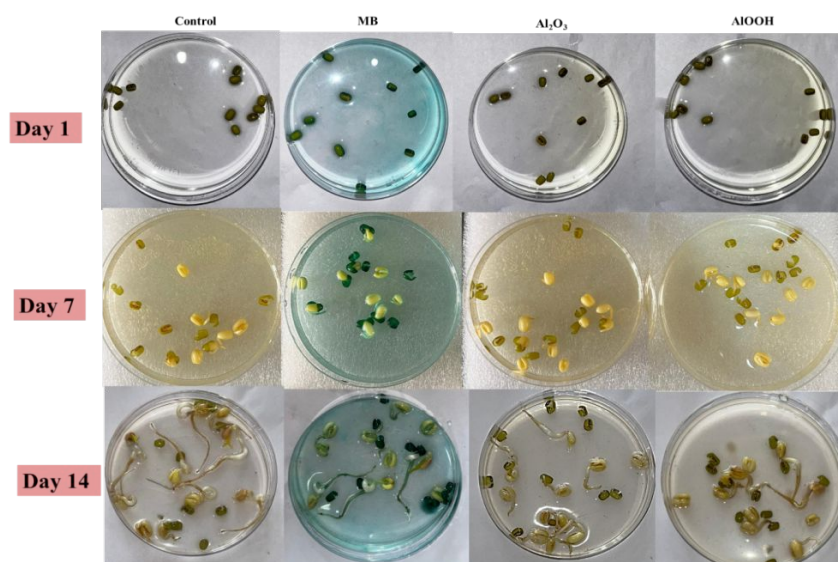


**Figure 9:** Mung seeds (*Vigna radiata*) growth in different conditions over two weeks (14 days)



Excellent results were seen in both  $\text{Al}_2\text{O}_3$  and  $\text{AlOOH}$  particles when tested for reusability. This assessment was performed under visible light conditions at pH 7. As seen in the initial graphs (**Figure 5**),  $\text{Al}_2\text{O}_3$  was able to degrade 99.29% of the MB dye, in the second cycle, the degradation efficiency was 97.09% and in the third cycle the degradation efficiency was 91.79%. The degradation of  $\text{AlOOH}$  followed a similar pattern (**Figure 5**), under light conditions indicating a 75.99% degradation. The second and third cycles then show a 74.47% and 75.78% degradation of MB, respectively (**Figure 10**).

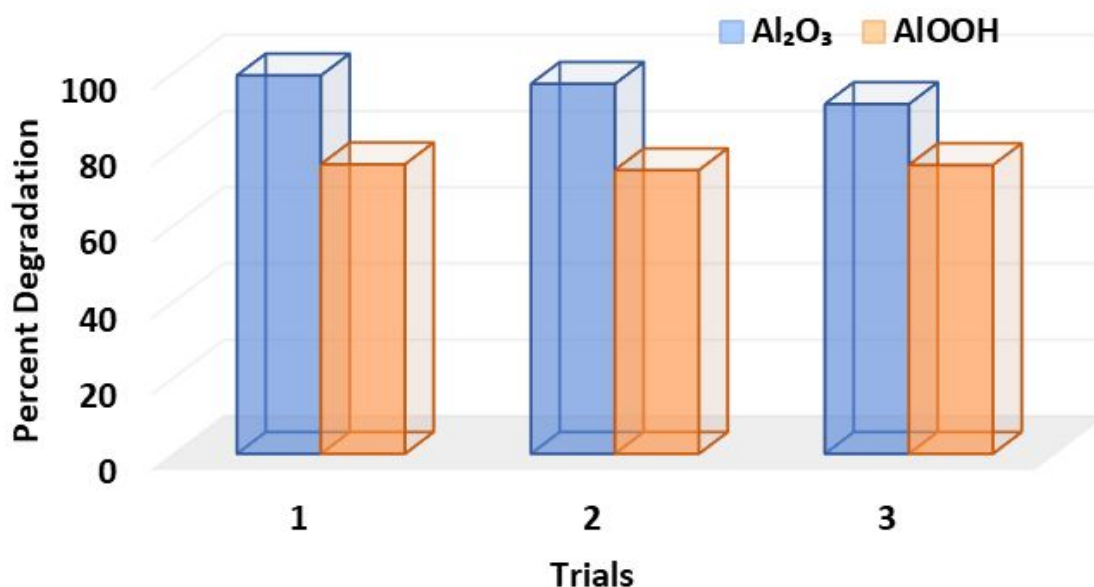


**Figure 10:** The graph of  $\text{Al}_2\text{O}_3$  and  $\text{AlOOH}$  after three cycles of using, drying, and reusing.

A comparative study was used to assess the degradation efficiency of various metal oxide nanoparticles in different dyes. Dyes including malachite green, brilliant crystal, methylene blue, and methylene were examined [15]. The findings of this comparison revealed that the synthesized  $\text{Al}_2\text{O}_3$  exhibited the highest effectiveness in degrading the MB dye.

**Table 4:** Analysis of photocatalytic efficiencies of various metal oxides, dye, time, and degradation percentages.



Metal oxide NPs	Photocatalyst amount	Concentration of Dye	Dye	Degradation Time (min) (light source)	Degradation Percent (%)	Ref
Al <sub>2</sub> O <sub>3</sub> prepared by sol-gel method γ-Al <sub>2</sub> O <sub>3</sub> prepared by precipitation 14method	10 mg	0.01 mM of MB	MB	240 (Sunlight)	sol-gel-Al <sub>2</sub> O <sub>3</sub> : 85.0 % γ-Al <sub>2</sub> O <sub>3</sub> : 91.6%	14
Al <sub>2</sub> O <sub>3</sub>	100 mg	1.5 × 10 <sup>-5</sup> mol/L	Malachite green	360 (Sun light)	45%	48
γ- Al <sub>2</sub> O <sub>3</sub> NP	60 mg	20 PPM	MB	60 (UV light)	96.4 %	49
N-ZnO	50 mg	100 mL of MB 20 mg/L	MB	80 (solar-simulated light)	95.3%	50
MnFe <sub>2</sub> O <sub>4</sub>	30 mg	10 PPM	MB	290 (UV light)	97%	51
Al <sub>2</sub> O <sub>3</sub> /SiO <sub>2</sub>	300 mg	-	Malachite green	300 (sun light)	85%	52
Al <sub>2</sub> O <sub>3</sub> /Fe <sub>2</sub> O <sub>3</sub>	200 mg	100 mL of MB solution (25 mg/L)	MB	90 (visible light)	75.1%	53
Biosynthesized ZnO	20 mg	2.0 × 10 <sup>-5</sup> M	MB	420 (visible light)	98%	54



AlOOH	50 mg	5 PPM	MB	240 (visible light)	75.99%	Current
Al <sub>2</sub> O <sub>3</sub>	50 mg	5 PPM	MB	240 (visible light)	99.29%	Current

**Table 4** provides a comprehensive summary of Al<sub>2</sub>O<sub>3</sub> and other metal oxides prepared by various methods that have been used for photocatalytic degradation under different light sources. As shown in the table, the MB degradation efficiencies are comparable with the irradiation times in many studies. However, some results differ from the findings of this paper due to variations in the synthesis processes and the use of different light sources, such as sunlight and UV illumination. Unlike previous studies, where Al<sub>2</sub>O<sub>3</sub> was prepared electrochemically [49] or from aluminum salts like aluminum nitrate and sodium hydroxide [48], our novel study uses waste aluminum foil for a green synthesis of the particles. The Al<sub>2</sub>O<sub>3</sub> and AlOOH synthesized in this manner can serve not only as photocatalysts but also in various other industries and processes.

**Conclusion:** This study successfully demonstrated that compromised foil can be reused to synthesize Al<sub>2</sub>O<sub>3</sub> and AlOOH particles that are effective photocatalysts for dye degradation. This comprehensive research analyzed the particle structure, shape, bonds, composition, thermal stability, degradation efficiency, toxicity, and reusability. The particles were observed at neutral, basic, and acidic conditions. The results convey that the MB degradation was most efficient in the light for any pH considered. The experiments further revealed that in the light, the highest efficiency was observed when using Al<sub>2</sub>O<sub>3</sub> under neutral conditions, achieving a degradation



efficiency of 99.29%. Additionally, the highest efficiency was achieved in the light with AIOOH under acidic conditions, with a degradation efficiency of 86.67%. It was also observed that the pH conditions affect the degradation of the dye solution in both light and dark. Moreover, it was observed that in the dark, the absorbance of the dye decreased initially and then stabilized while there was a constant decrease in the absorbance of the dye in the light. This proved that the MB dye is primarily absorbed in the dark but degraded in the light. The toxicity results further revealed that control,  $\text{Al}_2\text{O}_3$ , AIOOH, and MB produced the most germinated seeds, respectively. The germination indexes of the solutions were observed in the following order: control,  $\text{Al}_2\text{O}_3$ , MB, and AIOOH. The toxicity assessment also proved that these particles could degrade MB in bulk reactions. Both particles also showed remarkable recyclability for at least three cycles.

**Conflicts of interest:** There are no conflicts to declare.

**Data availability:** Data supporting this study are included within the article and/or supporting materials

**Acknowledgment:** G. R. Chaudhary is also thankful Department of Science and Technology (DST)-Water Technologies Cell for Project No. WTC/OWUIS-2021/TS-04 (G). B. Sharma is thankful to DST Inspire SRF (IF170098) and the Commonwealth Scholarship Commission (CSC) (INCN-2019-409). All authors are thankful to SAIF/CIL, Panjab University for providing characterization facilities.

**Conflicts of interest:** There are no conflicts to declare.

## References

- [1] W. L. Filho, A. L. Salvia, A. Minhas, A. Paço, & C. Dias-Ferreira, *Sci. Total Environ.*, 2021, **770**, 145257



- [2] D. Winton, L. Marazzi, & S. Loiseau, *Sci. Total Environ.*, 2022, **820**, 153229.
- [3] G. L. Robertson, *Elsevier*, 2019
- [4] L Mahmudah and S R Juliastuti, *IOP Conf. Ser.: Earth Environ. Sci.*, 2023, **1239**, 012011
- [5] N. A. Ghulam, M. N. Abbas and D. E. Sachit, *Int. J. Innov. Sci. Res. Technol.*, 2019, **4**,326-331
- [6] G. V. Calder & T. D. Stark, *Pract. Period. Hazard. Toxic. Radioact. Waste Manage.*, 2010, **14(4)**, 258-265
- [7] M. Mold, C. Linhart, J. Gómez-Ramírez, A. Villegas-Lanau, & C. Exley, *J. Alzheimers Dis.*, 2020, **76(3)**, 725-732
- [8] E. P. Meshcheryakov, S. I. Reshetnikov, M. P. Sandu, A. S. Knyazev and I. A. Kurzina, *Appl. Sci.*,2021,**11(6)**, 2457
- [9] A. Mukherjee, I. Mohammed, Tc. Prathna. and N. Chandrasekaran, *Sci. Against Microb. Pathog.:Commun. Curr. Res. Technol. Adv.*,2011, **1**, 245-251.
- [10] V. S. Saji, T. Kumeria, K. Gulati, M. Prideaux, S. Rahman, M. Alsawat, A. Santos, G. J. Atkinsb and D. Losic, *J. Mater. Chem. B*, 2015, **3(42)**, 8376-8388
- [11] U. Chakraborty, G. Kaur, H.-G. Rubahn, A. Kaushik, G. R. Chaudhary, & Y. K. Mishra, *Prog. Mater. Sci.*, 2023, **139**, 101169
- [12] A. Singh, J. Dhau, R. Kumar, R. Badru, P. Singh, Y. Kumar Mishra, A. Kaushik, *Prog. Mater. Sci.*, 2024, **144**, 101289. (b) N. G. Macedo, J. C. Alvim, L. C. Soares, L. S. da Costa, M. T. Galante, V. S. Lima and C. Longo, *Mater. Adv.*, 2024, **5**, 4541-4562
- [13] N. Tyagi, G. Sharma, D. Kumar, P. P. Neelratan, D. Sharma, M. Khanuja, M. K. Singh, V. Singh, A. Kaushik, S. K. Sharma, *Coord. Chem. Rev.*, 2023, **496**, 215394.
- [14] N. O. Eddy, R. A. Ukpe, R. Garg, R. Garg, A. Odiongenyi, P. Ameh, I. N. Akpet, S. E. Udo, *Clean Technol. Environ. Policy*, 2023,1-32.
- [15] F. I. Sangor and M. A. Al-Ghouti, *Case Stud. Chem. Environ. Eng.*, 2023, **8**, 100394
- [16] K. K. Anna, N. K. R. Bogireddy, V. Agarwal and R. R. Bon, *Mater. Lett.*, 2022, **317**,132085



- [17] A. U. Ezeibe, E. C. Nleonu, C. C. Onyemenonu, N. Arrousse, C. C Nzebunachi, *Saudi J. Eng. Technol.*, 2022, **7**, 132-136
- [18] S. Zhang, I. Khan, X. Qin, K. Qi, Y. Liu, S. Bai, *Front. Chem.* 2020, **8**, 117
- [19] Q. Liu, *IOP Conf. Ser.: Earth Environ. Sci.*, 2020, **514**, 052001
- [20] A. M. Chauhan, A. B. Sharma, R. Kumar, G. R. Chaudhary, A. A. Hassan., S. Kumar, *Environmental Research*, 2019, **168**, 85-95
- [21] S. Mondal, *Env. Eng. Sci*, 2008, **25**, 295–308.
- [22] H. Zou, W. Ma and Y. Wang, *Arch. Environ. Prot.* 2015, **41**, 33-39
- [23] R. J. Ganaie, S. Rafiq, A. Sharma, *IOP Conf. Ser.: Earth Environ. Sci.*, 2023, **1110**, 4-9
- [24] F. M. D. Chequer, G. A. R. de Oliveira, E. R. A. Ferraz, J. C. Cardoso, M. V. B. Zanoni, and D. P. de Oliveira, 2013, **151**
- [25] K. Saravanan, B. Shanthi, C. Ravichandran, B. Venkatachalapathy, K. I. Sathiyarayanan, S. Rajendran, N. S. Karthikeyan and R. Suresh, *Environmental Research*, 2023, **218**, 114985
- [26] A. Mitelut and M. E. Popa, *Roman. Biotechnol. Lett.* 2011, **16(1)**, 121-129
- [27] M. N. Nduni, A. M. Osano and B. Chaka, *Clean. Eng. Technol*, 2021, **3**, 100108
- [28] R. R. Toledo, V. R. Santoyo, D. M. Sánchez and M. Martínez, *N. Sci.*, 2018, **10**, 1217
- [29] C. Yua, Z. Li, L. Zhou and G. Ju, *Materials (Basel)*, 2022, **15(6)**, 2169
- [30] Y. Yang, Y. Xu, B. Han, B. Xu, X. Liu and Z. Yan, *J. Colloid Interface Sci*, 2022, **469**, 1-7
- [31] M. A. Ates, V. Demir, Z. Arslan, J. Daniels, I. O. Farah and C. Bogatu, *Environmental Toxicology*, 2013, **30(1)**, 109–118
- [32] S. Pakrashi, S. Dalai, A. Humayun, S. Chakravarty, N. Chandrasekaran and A. Mukherjee, *PloS one*, 2015, **8(9)**, 74003
- [33] N. Bao, X. Miao, X. Hu, Q. Zhang, X. Jie and X. Zheng, *Catalysis*, 2017, **7**, 117



- [34] S. A. Ansari and Q. Husain, *J. Mol. Catal. B: Enzymatic*, 2011, **70 (3-4)**, 119-126
- [35] T.-Z. Ren, Z.-Y. Yuan and B.-L. Su, *ACS Publications*, 2004, **20(4)**, 153
- [36] A. Baccarella, R. Garrard, M. Beauvais, U. Bednarski, S. Fischer, A. Abeykoon, K. Chapman, B. Phillips, J. Parise and J. Simonson, *J. Solid State Chem.*, 2021, **301**, 1
- [37] S. I. Al-nassar, A. K. M. and Z. F. Mahdi, *Manuf. Sci. Technol.*, 2015, **3(4)**, 79
- [38] X. Zhou, J. Zhang, Y. Ma, H. Tian, a. L. Que Wang and L. J. Q. Cu, *RSC Adv.*, 2017, **7**, 4907
- [39] E. O. Filatova and A. S. Konashuk, *J. Phys. Chem. C*, 2015, **119(35)**, 20755–20761
- [40] F. Tzompantzi, Y. Piña, A. Mantilla, O. A. Martínez, F. G. Hernández, X. Bokhimi, and A. Barrera, *Catal. Today*, 2014, **220-222**, 49-55
- [41] X. Yan, K. Yuan, N. Lu, H. Xu, S. Zhang, N. Takeuchi, H. Kobayashi, and R. Li, *Appl. Catal. B: Environ.*, 2017, **218(5)**, 20-31
- [42] K. Edalati, I. Fujita, S. Takechi, Y. Nakashima, K. Kumano, H. R. Khosroshahi, M. Arita, M. Watanabe, X. Sauvage, T. Akbay, T. Ishihara, M. Fuji, and Z. Horita, *Scr. Mater.*, 2019, 173, 120-124
- [43] K.B. Kusuma, M. Manju, C.R. Ravikumar, H.P. Nagaswarupa, M.A.S. Amulya, M.R. Anilkumar, B. Avinash, K. Gurushantha, N. Ravikantha, *Sensors Int.*, 2020, **1**, 100039
- [44] M.A Gondal, T.A Fasasi, A. Mekki, and T.A. Saleh., *Nanosci. and Nanotech. Letters*, 2016, 8(1), 17-25
- [45] Small, J. M., & Hintelmann, H. (2007). *Analytical and bioanalytical chemistry*, **387**, 2881-2886.
- [46] Jia, P., Tan, H., Liu, K., & Gao, W. (2018). *Materials Research Bulletin*, **102**, 45-50.
- [47] M. Chauhan, B. Sharm, R. Kumar, G. R. Chaudhary, A. A. Hassan and S. Kumar, *Environmental Research*, 2019, **168**, 85-95.
- [48] D. Pathania, R. Katwal, H. Kaur, *Int. J. Miner. Metall. Mater.*, 2016, 23, 358–371.





- [49] K.B. Kusuma, M. Manju, C.R. Ravikumar, H.P. Nagaswarupa, M.A.S. Amulya, M.R. Anilkumar, B. Avinash, K. Gurushantha, N. Ravikantha, *Sensors Int.*, 2020, **1**, 100039
- [50] L. Sun, Q. Shao, Y. Zhang, H. Jiang, S. Ge, S. Lou, J. Lin, J. Zhang, S. Wu, M. Dong, Z. Guo, *J. Colloid Interface Sci.*, 2020, **565**, 142–155
- [51] B. Mandal, J. Panda, P. K. Paul, R. Sarkar, B. Tudu, *Vacuum.*, 2020, **173**, 109150
- [52] T. Ali, C.P. Mahesh, M. Sharon, M. Sharon, *IJESRT*, 2018, **7**, 603-608
- [53] H. Hassena, *Mod. Chem. Appl.*, 2016, **4**, 3–7
- [54] F. H. Abdullah, N. H. H. Abu Bakar, M. Abu Bakar, *Optik.*, 2020, **206**, 164279



## Data availability

Data supporting this study are included within the article and/or supporting materials.

